

# Dark Energy Anisotropic Stress and Large Scale Structure Formation

Tomi Koivisto<sup>1\*</sup> and David F. Mota<sup>2†</sup>

<sup>1</sup> *Helsinki Institute of Physics, FIN-00014 Helsinki, Finland and*

<sup>2</sup> *Institute of Theoretical Astrophysics, University of Oslo, Box 1029, 0315 Oslo, Norway*

(Dated: October 20, 2019)

We investigate the consequences of an imperfect dark energy fluid on the large scale structure. A phenomenological three parameter fluid description is used to study the effect of dark energy on the cosmic microwave background radiation (CMBR) and matter power spectrum. In addition to the equation of state and the sound speed, we allow a nonzero viscosity parameter for the fluid. Then anisotropic stress perturbations are generated in dark energy. In general, we find that this possibility is not excluded by the present day cosmological observations. In the simplest case when all of the three parameters are constant, we find that the observable effects of the anisotropic stress can be closely mimicked by varying the sound speed of perfect dark energy. However, now also negative values for the sound speed, as expected for adiabatic fluid model, are tolerable and in fact could explain the observed low quadrupole in the CMBR spectrum. We investigate also structure formation of imperfect fluid dark energy characterized by an evolving equation of state. In particular, we study models unifying dark energy with dark matter, such as the Chaplygin gas or the Cardassian expansion, with a shear perturbation included. This can stabilize the growth of inhomogeneities in these models, thus somewhat improving their compatibility with large scale structure observations.

PACS numbers: 98.80.-k, 98.80.Jk

Keywords: Cosmology: Theory, Large-Scale Structure of Universe

## I. INTRODUCTION

Dark energy is a fundamental component of the nowadays standard cosmological model. It would be very difficult to explain the set of present days cosmological observations without it. Specifically, we refer to the luminosity-redshift relationship from observations of supernovae of type Ia (SNIa) [1, 2, 3], the matter power spectrum of large scale structure as inferred from galaxy redshift surveys like the Sloan Digital Sky Survey (SDSS) [4] and the 2dF Galaxy Redshift Survey (2dFGRS) [5], and the anisotropies in the Cosmic Microwave Background Radiation (CMBR) [6].

Despite of its major importance in explaining the astrophysical data, the nature of dark energy is one of the greatest mysteries of modern cosmology. The simplest and most popular candidates for it are the cosmological constant (see e.g. [7]), and minimally coupled scalar fields (see e.g. [8, 9, 10, 11]). However many other candidates were proposed based on high energy physics phenomenology ( see e.g. [12, 13, 14, 15, 16, 17, 18, 19, 20, 21, 22]), and many investigations on their possible astrophysical and cosmological signature were undertaken ( see e.g. [23, 24, 25, 26, 27, 28, 29, 30, 31, 32, 33, 34, 35]).

With so many possible candidates it is imperative to understand what are the main properties of the dark energy component that could have specific signatures in the astronomical data, and so could help us to discriminate

among all these models.

In a phenomenological approach, dark energy might be mainly characterized by its equation of state  $w$ , its sound speed  $c_s$ , and its anisotropic stress  $\sigma$  [36]. Much effort has been put into determining the equation of state of dark energy, in an attempt to constrain theories. The equation of state determines the decay rate of energy and thus affects both the background expansion and the evolution of matter perturbations (see e.g [37]). An equally insightful characteristic of dark energy is its speed of sound. This does not affect the background evolution but is fundamental in characterizing the behavior of its perturbations. Hence many authors have explored its effect on the evolution of fluctuations in the matter distribution ( see e.g. [38, 39, 40, 41]). However, the investigation of the effects of the anisotropic stress has been widely neglected.

The main reason for disregarding the anisotropic stress in the dark energy fluid might be that conventional dark energy candidates, such as the cosmological constant or scalar fields, are perfect fluids with  $\sigma = 0$ . However, since there is no fundamental theoretical model to describe dark energy, there are no strong reasons to stick to such assumption. In fact, dark energy vector field candidates have been proposed [42, 43, 44, 45, 46], and these have  $\sigma \neq 0$ . Of course, if dark energy is such a vector, one might break the isotropy of a Friedmann-Robertson-Walker universe. However, as long as it remains subdominant, this violation is likely to be observationally irrelevant [47]. Once dark energy comes to dominate though, one would expect an anisotropic expansion of the universe, in conflict with the significant isotropy of the CMBR [48]. But on the other hand there appears to be hints of statistical anisotropy in the CMBR fluctuations

---

\*tomikoiv@pcu.helsinki.fi

†mota@astro.uio.no

[49, 50, 51, 52, 53, 54].

Recently the possibility of viscous dark energy has gained attention [55, 56, 57, 58]. These models are usually restricted to the context of bulk viscosity, although one could expect the shear viscosity to be dominant [58]. One can allow bulk viscosity in a Friedmann-Robertson-Walker (FRW) universe, but when the shear is not neglected one has to face the difficulties of an anisotropic universe. However, shear viscosity at the perturbative level is compatible with the assumption of an isotropic FRW background. In fact the anisotropic stress perturbation is crucial to the understanding of evolution of inhomogeneities in the early, radiation dominated universe. Therefore an obviously interesting question is whether present observational data could allow for an anisotropic stress perturbation in the late universe which is dominated by the mysterious dark energy fluid.

Motivated by all these possibilities, we investigate if the possible existence of an anisotropic stress in the dark energy component would result in a specific cosmological signature which could be probed using large scale structure data, and if it would still be compatible with the latest CMBR temperature anisotropies and the matter power spectrum.

The article is organized as follows: In section II we discuss the parameters describing a general dark energy fluid with anisotropic stress. In section III we consider dark energy imperfect fluid models parameterized with a constant equation of state, sound speed and anisotropic stress. We investigate the effects on the late time perturbation evolution, in the integrated Sachs-Wolfe (ISW) effect of the CMBR anisotropies and on the matter power spectrum. In section IV we extend the analysis to models unifying dark energy with dark matter. We end the article with a summary of our findings and conclusions.

## II. DARK ENERGY STRESS PARAMETERIZATION

In its simplest descriptions the dark energy component is described fully by its equation of state, defined as

$$w \equiv \frac{p}{\rho}, \quad (1)$$

where  $\rho$  is the energy density and  $p$  is the pressure of the fluid. If  $u_\mu$  is the four-velocity of the fluid, and the projection tensor  $h_{\mu\nu}$  is defined as  $h_{\mu\nu} \equiv g_{\mu\nu} + u_\mu u_\nu$ , we can write the energy momentum tensor for a general cosmological fluid as

$$T_{\mu\nu} = \rho u_\mu u_\nu + p h_{\mu\nu} + \Sigma_{\mu\nu}, \quad (2)$$

where  $\Sigma_{\mu\nu}$  can include only spatial inhomogeneity. We define perfect fluid by the condition  $\Sigma_{\mu\nu} = 0$ . If in addition the fluid is adiabatic,  $p = p(\rho)$ , the evolution of its perturbations is described by the adiabatic speed of

sound  $c_a$ . This is in turn fully determined by the equation of state  $w$ ,

$$c_a^2 \equiv \frac{\dot{p}}{\dot{\rho}} = w - \frac{\dot{w}}{3H(1+w)}. \quad (3)$$

For an adiabatic fluid,  $\delta p = c_a^2 \delta \rho$ .

In the general case, there may be more degrees of freedom and the pressure  $p$  might not be a unique function of the energy density  $\rho$ . An extensively studied example is quintessence [8, 9, 10, 11]. For such a scalar field the variables  $w$  and  $c_s^2$  depend on two degrees of freedom: the field and its derivative, or equivalently, the kinetic and the potential energy of the field. Then the dark energy (entropic) sound speed is defined as the ratio of pressure and density perturbations in the frame comoving with the dark energy fluid,

$$c_s^2 \equiv \frac{\delta p}{\delta \rho|_{de}}. \quad (4)$$

In the adiabatic case,  $c_s^2 = c_a^2$ , which holds in any frame, but in general the ratio  $\delta p / \delta \rho$  is gauge dependent. Hence, in the case of entropic fluid such as scalar fields, one needs both its equation of state and its sound speed as defined in Eq. (4), to have a complete description of dark energy and its perturbations.

However, in order to have an even more general set of parameters to fully describe a dark energy fluid and its perturbations, besides  $w$  and  $c_s$ , one should also consider the possibility of anisotropic stress. This is important because it enters directly into the Newtonian metric, as opposed to  $w$  and  $c_s$  which only contribute through the causal motion of matter [36].

Taking this generalization into account, in the synchronous gauge [59], the evolution equations for the dark energy density perturbation and velocity potential can be written as [60]

$$\begin{aligned} \dot{\delta} &= -(1+w) \left\{ [k^2 + 9H^2(c_s^2 - c_a^2)] \frac{\theta}{k^2} + \frac{\dot{h}}{2} \right\} \\ &\quad - 3H(c_s^2 - w)\delta, \end{aligned} \quad (5)$$

$$\dot{\theta} = -H(1 - 3c_s^2)\theta + \frac{c_s^2 k^2}{1+w}\delta - k^2\sigma, \quad (6)$$

where  $h$  is the trace of the synchronous metric perturbation. Here  $\sigma$  is the anisotropic stress of dark energy, related to notation of Eq.(2) by  $(\rho + p)\sigma \equiv -(\hat{k}_i \hat{k}_j - \frac{1}{3}\delta_{ij})\Sigma^{ij}$ . Basically, while  $w$  and  $c_s^2$  determine respectively the background and perturbative pressure of the fluid that is rotationally invariant,  $\sigma$  quantifies how much the pressure of the fluid varies with direction.

Generally such a property implies shear viscosity in the fluid, and thus its effect is to damp perturbations. A covariant form for the viscosity generated in the fluid flow is [61]

$$\Sigma_{\mu\nu} = \varsigma (u_{\mu;\alpha} h_\nu^\alpha + u_{\nu;\alpha} h_\mu^\alpha - u^\alpha_{;\alpha} h_{\mu\nu}) + \zeta u^\alpha_{;\alpha} h_{\mu\nu}. \quad (7)$$

Now the the conservation equations  $T^{\mu\nu}_{;\mu} = 0$  reduce to the Navier-Stokes equations in the non-relativistic limit. Here  $\varsigma$  is the shear viscosity coefficient, and  $\zeta$  represents bulk viscosity. Here we set the latter to zero since we demand that  $\Sigma_{ij}$  is traceless. In cosmology we have  $u_\mu = (1, -v_i)/a$  in the synchronous gauge, and the velocity potential  $\theta$  is the divergence of the fluid velocity  $v$ . It is then straightforward to check that the components of Eq.(8) vanish except in the off-diagonal of the perturbed spatial metric. One finds that

$$\sigma = \frac{\varsigma}{k} \left( \theta - \dot{H}_T \right), \quad (8)$$

where  $H_T$  is the scalar potential of the tensorial metric perturbations, which in the synchronous gauge equals  $H_T = -h/2 - 3\eta$ , where  $\eta$  is a metric perturbation. From the coordinate transformation properties of  $T_{\mu\nu}$  it follows that  $\sigma$  must be gauge-invariant, and indeed the linear combination  $\theta - \dot{H}_T$  is frame-independent.

However, the anisotropic stress is not necessarily given directly by  $\theta - \dot{H}$ . For neutrinos this term instead acts as a source for the anisotropic stress, which is also coupled to higher multipoles in the Boltzmann hierarchy. Thus the evolution of the stress must, at least in principle, be solved from a complicated system of evolving multipoles.

The approach we will use in this article to specify the shear viscosity of the fluid is more in line with the neutrino stress than Eq.(8). Following Hu [62], we describe the evolution of the anisotropic stress with the equation

$$\dot{\sigma} + 3H \frac{c_a^2}{w} \sigma = \frac{8}{3} \frac{c_{vis}^2}{1+w} \left( \theta + \frac{\dot{h}}{2} + 3\dot{\eta} \right). \quad (9)$$

Then the shear stress is not determined algebraically from fluctuations in the fluid as was the case in Eq. (8), but instead it must be solved from a differential equation.

This phenomenological set-up is motivated as follows [36]. One can guess that the anisotropic stress is sourced by shear in the velocity and in the metric fluctuations. Again one must take into account the coordinate transformation properties of  $\sigma$ , and construct a gauge-invariant source term in the differential equation. As mentioned, an appropriate linear combination is  $\theta - \dot{H}_T$ . Up to the viscosity parameter  $c_{vis}^2$ , this determines the right hand side of Eq. (9). In the left hand side there appears also a drag term accounting for dissipative effects. We have adopted a natural choice for the dissipation time-scale,  $\tau_\sigma^{-1} = 3H$ .

One may then check that Eq. (9) with  $w = c_{vis}^2 = 1/3$  reduces to the evolution equation for the massless neutrino quadrupole in the truncation scheme where the higher multipoles are neglected [59] (this applies also to photons when one ignores their polarization and coupling to baryons). In what follows, we will study the consequences of Eq.(9) for fluids with negative equations of state. For  $w < -1$ , one should consider negative values of  $c_{vis}^2$ , as was suggested in Ref. [63]. So the parameter  $c_{vis}^2/(1+w)$  should remain positive. We will return to this in the section III.C.

Note that the parameterization of Eqs.(5), (6) and (9) describes cosmological fluids in a very general way. The system reduces to cold dark matter equations when  $(w, c_s^2, c_{vis}^2)$  is  $(0, 0, 0)$  and relativistic matter corresponds to  $(1/3, 1/3, 1/3)$ . A scalar field with a canonical kinetic term is given by  $(w(a), 1, 0)$ , where  $-1 < w(a) < 1$ . With an arbitrary kinetic term one can construct k-essence models [17] characterized by unrestricted equations of state and speeds of sound,  $(w(a), c_s^2(a), 0)$ , but vanishing shear. On the other hand, one should keep in mind that the parameterization cannot be completely exhaustive. It does not cover, for example, a cosmological fluid with anisotropic stress determined by Eq. (8) when  $\varsigma \neq 0$ . We might address the viability of this approximation elsewhere, but restrict here to the parameterization given in Eq.(9).

### III. STRESSED DARK ENERGY FLUID

We will investigate the effect of dark energy perturbations on the CMBR anisotropies and on the matter power spectrum with the simplest assumption that all of the three parameters  $w$ ,  $c_s^2$  and  $c_{vis}^2$  are constant. This is an accurate description for a wide variety of models for which these parameters can be well approximated at moderate redshifts by their time-averaged values.

For the energy content of the universe we use  $\Omega_b = 0.044$ ,  $\Omega_{cdm} = 0.236$ ,  $\Omega_{de} = 0.72$  and  $h_0 = 0.68$ . In all the numerical calculations we assume a scale invariant initial power spectra and set optical depth to last scattering to zero. We normalize the perturbation variables by setting the primordial comoving curvature perturbation to unity. To compare with observations, the resulting power spectra must then be multiplied by the primordial amplitude of the curvature perturbation. For this we employ the same normalization for all the models considered in this article. Although we do not search for the best-fit models here, we include the WMAP data [6] and the SDSS data [4] in to the figures in order to give an idea about the viability of the studied models. The WMAP error bars include the cosmic variance, which is the dominant source of uncertainty for the small  $\ell$ 's. The calculations are performed with a modified version of the CAMB code [64].

In addition to specifying the cosmological parameters and the evolution equations (5), (6) and (9), we must address the initial conditions in the early universe. For the relative entropy between radiation and dark energy to vanish, one must impose

$$\begin{aligned} \delta &= \frac{3}{4}(1+w)\delta_r, \\ \theta &= \frac{1}{1+9\frac{H^2}{k^2}(c_s^2 - c_a^2)} \left[ \theta_r - \frac{9}{4}H(c_s^2 - c_a^2)\delta_r \right]. \end{aligned} \quad (10)$$

When there is no inherent entropy in the dark energy fluid, i.e.  $c_s^2 = c_a^2$ , adiabaticity means that the velocity

potentials of all cosmic fluids are equal. On the other hand, when  $c_s^2 \neq c_a^2$ , we see that the above condition implies that the dark energy velocity potential is negligible in the early universe, since the relevant scales are far outside the horizon,  $k \ll H$ . However, the condition that the relative entropy Eq.(10) vanishes, when  $c_a^2 = c_s^2$ , would be strictly valid only for the instant that it is imposed. Thereby, although there is some arbitrariness in the choice of initial values, the late evolution is not affected by the choice of these values as long as they are inside some reasonable region. We use, for all models, the initial values

$$\delta = \frac{3}{4}(1+w)\delta_r, \quad \theta = \theta_r, \quad \sigma = 0. \quad (11)$$

The two first initial conditions are derived assuming that  $c_s^2 = c_a^2$  and that the relative entropy between dark energy and radiation together with its first derivatives vanishes. The third condition says that we set the anisotropic stress to zero at very large scales at an early time. Only then shear is not generated when  $c_{vis}^2 = 0$ . Thus fluids with vanishing viscous parameter are perfect. Note however that when the parameter is allowed to evolve with time, one can have  $c_{vis}^2 = 0$  for an imperfect fluid at some stage.

### A. Dark Energy models with $-1 < w < 0$

When  $w$  is negative but larger than  $-1$ , the evolution of perturbations is determined by the two sound speeds of dark energy. The evolution has been analyzed in Ref. [65] but without including the anisotropic stress.

The metric perturbation  $h$  is now a source in Eq. (5), which tends to draw dark energy into overdensities of cold dark matter. However, for large scales the source due to velocity perturbations is proportional to  $-(1+w)(c_s^2 - w)\theta/k^2$ , and this term can dominate the metric source term and drive  $\delta$  to smaller values. In fact  $\delta$  drops below zero when evaluated in the synchronous gauge<sup>1</sup>. This happens especially for large sound speeds, since then both the friction term in Eq. (6) and the source term in Eq. (5) are larger (see FIG. 1). Thus  $\delta$  gets smaller when dark energy begins to dominate. The ISW effect is enhanced when one increases the sound speed squared.

The effect of the anisotropic stress is also to wash out overdensities. This is because the metric part of the source term in Eq. (9) turns out negative, and it dominates over the velocity term. Thus  $\sigma$  is driven to negative values, and in Eq. (6) it will act to increase the growth of  $\theta$ . This is similar to free-streaming of neutrinos, although for them the effect is relevant at smaller scales.

<sup>1</sup> More accurately, we evaluate the transfer functions of the perturbations. A negative value for the transfer function indicates that a perturbation variable acquires the opposite sign to its initial value.

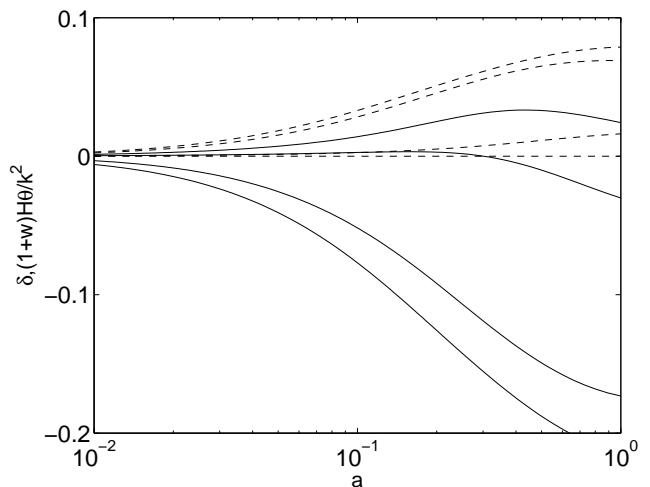


FIG. 1: Late evolution of the dark energy density perturbation and velocity potential for  $k = 1.3 \cdot 10^{-4} \text{ Mpc}^{-1}$  when  $w = -0.8$ . Solid lines from top to bottom correspond to  $\delta$ , and dashed lines from bottom to top correspond to  $(1+w)H\theta/k^2$  when  $(c_s^2, c_{vis}^2) = (0,0), (0.6,0), (0,0.6), (0.6,0.6)$ . The effect of  $c_{vis}^2$  is to damp density perturbations, which in the synchronous gauge is seen as a consequence of enhancing the velocity perturbations.

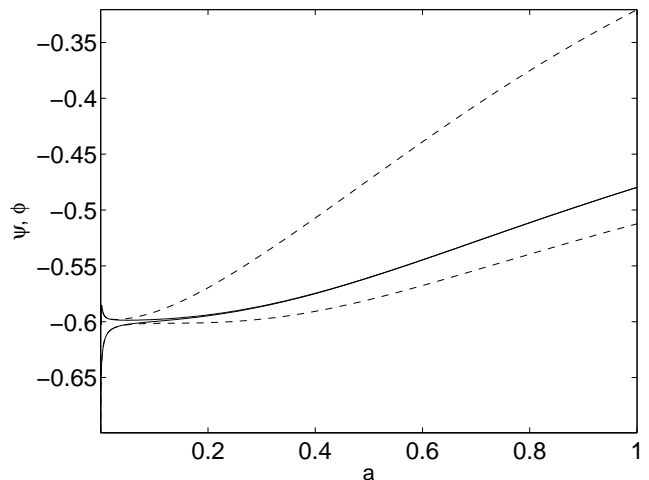


FIG. 2: Late evolution of the gravitational potentials at large scales ( $k = 1.3 \cdot 10^{-4} \text{ Mpc}^{-1}$ ) when  $w = -0.8$  and  $c_s^2 = 0$ . Solid lines are for the case of perfect dark energy and dashed for the imperfect case with  $c_{vis}^2 = 1.0$ . The upper lines are  $\psi$ , the lower lines are  $\phi$ .

Since now  $c_a^2 < 0$ , the source term  $\sim H^2\theta/k^2$  in Eq. (5) inhibits structure growth at large scales. Therefore, as the dark energy becomes dominant, the overall density structure is smaller when  $c_{vis}^2$  is larger, and the ISW effect is amplified.

It is illuminating to describe the same thing also in terms of the Newtonian gauge perturbations. This gauge

is defined by the line element

$$ds^2 = a^2(\tau) [-(1 + 2\phi)d\tau^2 + (1 - 2\psi)dx^i dx_i]. \quad (12)$$

Here  $\tau$  is the conformal time. We remind that the ISW effect stems from the time variation of the metric fluctuations,

$$C_\ell^{ISW} \propto \int \frac{dk}{k} \left[ \int_0^{\tau_{LSS}} d\tau (\dot{\phi} + \dot{\psi}) j_\ell(k\tau) \right]^2, \quad (13)$$

where  $\tau_{LSS}$  is the conformal distance to the last scattering surface and  $j_\ell$  the  $\ell$ 'th spherical Bessel function. The ISW effect occurs because photons can gain energy as they travel through time-varying gravitational wells. These wells are in turn caused by matter, since

$$-k^2\phi = 4\pi G a^2 \rho \left[ \delta + 3 \frac{H}{k^2} (1+w)\theta \right]_{|T}. \quad (14)$$

We have indicated with the subscript  $|_T$  that in the left hand side variables refer to all matter present, and not just dark energy. Note also that the term in square brackets is gauge-invariant. Thus, evaluated in any frame, it equals  $\delta_T$ , the overdensity of energy seen in the comoving frame. During matter domination,  $\delta_T$  grows in such a way that the gravitational potentials stay constant. It is then clear that as dark energy begins to take over, the gravitational potential  $|\phi|$  begins to decay. Contrary to expectations from FIG. 1, this decay is not more efficient at large scales when there is shear, as shown in FIG. 2. This is because the dark energy shear influences gravitational wells in such a way that the growth of matter perturbations does not slow down as much as in a perfect universe.

However, there is an important twist to the story. This is seen in the FIG. 2, where the evolution of the potentials  $\phi$  and  $\psi$  is plotted at very large scales. At an early time the potentials are unequal because of the free streaming of radiation. However, our attention is now on the late evolution of the potentials. Due to dark energy, the potentials can re-depart from each other at smaller redshifts. This can happen only when  $c_{vis}^2 \neq 0$ , since

$$\psi = \phi - 12\pi G a^2 (1+w)\rho\sigma|_T, \quad (15)$$

i.e. shear is the difference between the depth of matter-induced gravity well and the amount of spatial curvature. Since  $\sigma$  is gauge-invariant, and we found that it becomes negative for dark energy, we can see that shear perturbation drives  $|\psi|$  to vanish more efficiently. Thereby we find that the effect of shear on Eq.(14) only partly compensates for the effect on  $\psi$  from Eq.(15), and thus the overall ISW from Eq.(13) will be amplified when dark energy perturbations tend to smooth as in FIG. 1.

In FIG. 3 we show the large angular scales of the CMBR spectrum when  $w = -0.8$  and the two other parameters are varied. The upper panel depicts the case where the sound speed of dark energy vanishes. Then

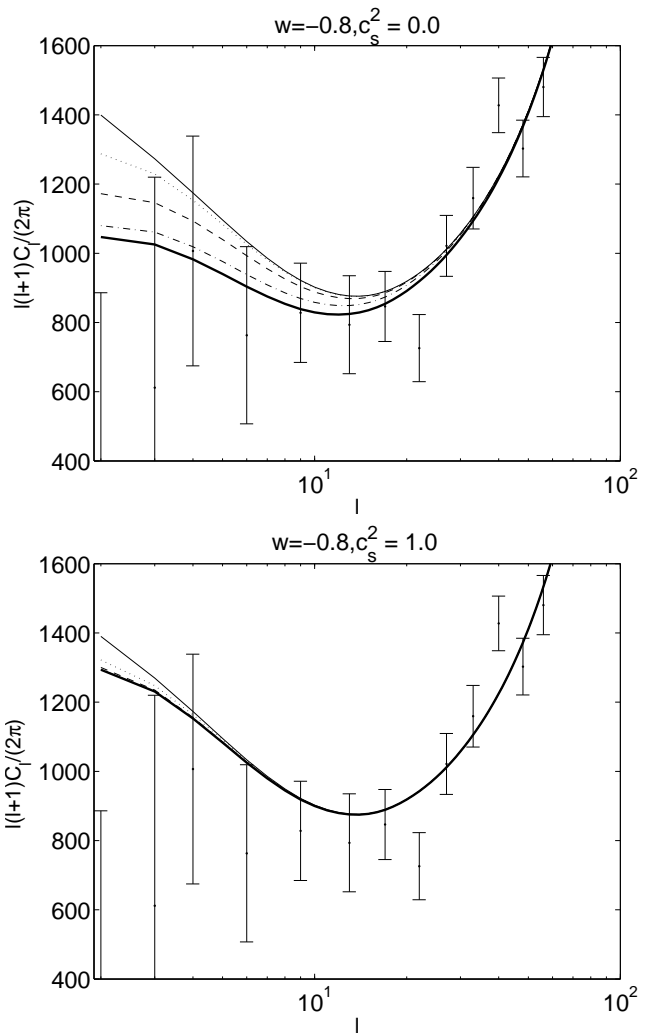


FIG. 3: The CMBR anisotropies for  $w = -0.8$ . In the upper panel  $c_s^2 = 0$  and in the lower panel  $c_s^2 = 1.0$ . The ISW contribution increases with the parameter  $c_{vis}^2$ : thick lines are for  $c_{vis}^2 = 0$ , dash-dotted for  $c_{vis}^2 = 0.001$ , dashed for  $c_{vis}^2 = 0.01$ , dotted for  $c_{vis}^2 = 0.1$  and the solid lines for  $c_{vis}^2 = 1.0$ .

the pressure perturbation vanishes and the clustering of dark energy is inhibited only by the free-streaming effect of shear viscosity. Therefore the large scale power of the CMBR is increased by increasing  $c_{vis}^2$ . In the lower panel  $c_s^2 = 1$ . Then dark energy is almost smooth (except at the largest scales) even without anisotropic stress, and thus we see a smaller effect when  $c_{vis}^2$  is increased.

When  $c_{vis}^2 < 0$  the metric and the fluid sources drive the perturbations in the same direction, resulting in explosive growth. Since this would spoil the evolution except when  $c_{vis}^2$  is tuned to infinitesimal negative values, we will not consider such a case here.

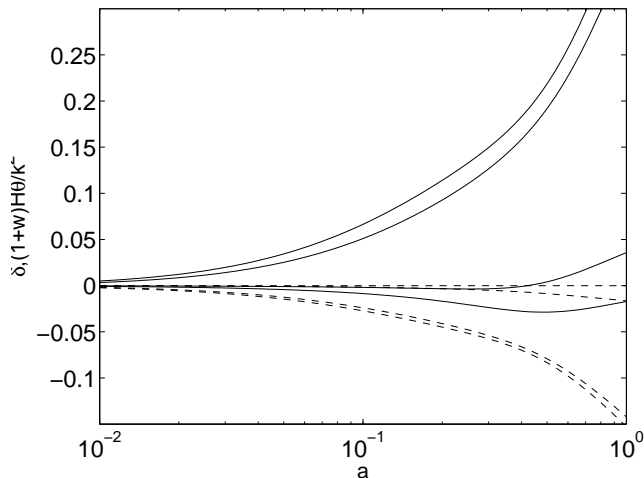


FIG. 4: Late evolution of the dark energy density perturbation and the velocity potential for  $k = 1.3 \cdot 10^{-4} \text{ Mpc}^{-1}$  when  $w = -1.2$ . Solid lines from bottom to top correspond to  $\delta$ , the dashed lines from top to bottom correspond to  $(1+w)H\theta/k^2$  when  $(c_s^2, c_{vis}^2) = (0,0), (0.6,0), (0,-0.6), (0.6,-0.6)$ . The effect of  $c_{vis}^2$  is to increase clustering, which in the synchronous gauge is seen as a consequence of enhancing the velocity perturbations.

### B. Phantom Dark Energy models with $w < -1$

When the dark energy equation of state is less than  $-1$ , the effect of both the sound speed and of the viscosity parameter are the opposite to the previous case. Now the source term in Eq. (5) has its sign reversed, and because of that dark energy falls out from the overdensities. Similarly, the velocity potential acts now as a source for the overdensities. Therefore increasing the sound speed will drive dark energy to cluster more efficiently. Now the effect of  $c_{vis}^2 > 0$  is with the same sign of those of the metric sources, and therefore we must consider negative values for this parameter. Then, if we increase the parameter  $c_{vis}^2/(1+w)$ , the dark energy perturbations are growing more efficiently, as shown in FIG. 4. This is because  $\sigma$  is negative, just like in the previous case, and again tends to enhance the velocity potential. The crucial difference in the perturbation evolution for imperfect dark energy here as compared to the imperfect  $w > -1$  case is that more shear in the perturbations will result in more clumpy structure in the density of phantom dark energy.

One can again consider the ISW in the terms of the Newtonian gauge potentials, Eq.(13). The effect is not directly seen from the behaviour of  $\delta$  in FIG. 4, partly because of the different gauge and partly because the anisotropic stress induces a compensation on the other gravitational potential and thereby influences also the matter perturbation. This is shown in FIG. 5. The anticipated simple result (that the decay of the gravitational potentials is reduced since  $\delta$  is enhanced when there is

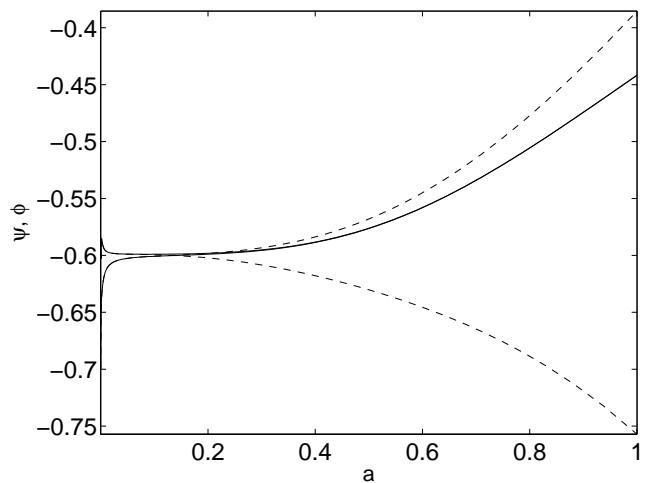


FIG. 5: Late evolution of the gravitational potentials at large scales ( $k = 1.3 \cdot 10^{-4} \text{ Mpc}^{-1}$ ) when  $w = -1.2$  and  $c_s^2 = 0$ . Solid lines are for the case of perfect dark energy and, dashed for the imperfect case with  $c_{vis}^2 = -1.0$ . The upper lines are  $\phi$ , the lower lines are  $\psi$ .

more shear) again holds for the sum of the gravitational potentials, but considering  $\phi$  or  $\psi$  separately reveals the intricacy of the fluctuation dynamics due to anisotropic stress. Again evolution of  $\phi$  implies, through Eq.(14), that the influence of  $\sigma$  to dark matter is the opposite from dark energy, but on the other hand, evolution of the spatial curvature  $\psi$  implies that the sum  $\phi + \psi$  behaves according to the dominating component. Now the gravitational well  $\psi$  grows deeper, because the contribution from shear in the phantom fluid in Eq.(15) comes with a minus sign.

In FIG. 6 we have plotted the large angular scales of the CMBR spectrum when  $w = -1.2$  and the two other parameters are varied. The upper panel depicts the case that the sound speed of dark energy vanishes. Then the ISW effect without anisotropic stress is large since dark energy perturbations are nearly washed out. Consequently, the large scale power of CMBR is decreased as  $|c_{vis}^2|$  is increased, since the "anti-viscosity" will then amplify perturbations. In the lower panel  $c_s^2 = 1$ . There the effect of  $c_s^2$  already dominates, and we see a smaller difference when  $c_{vis}^2/(1+w)$  is increased.

### C. Dark Energy models with $c_s^2 < 0$

For perfect dark energy models without shear, the case  $c_s^2 < 0$  leads to explosive growth of perturbations. This is analogous to the behaviour of a simple wave, which has a solution  $\sim e^{-i(k/c_s)t + i\vec{k}\cdot\vec{x}}$ , diverging when the sound velocity is imaginary. It is not clear, however, how useful the analogy to the sound speed of a simple plane wave is to the interpretation of the variable defined by Eq. (4). For instance, in the modified gravity context [33] this

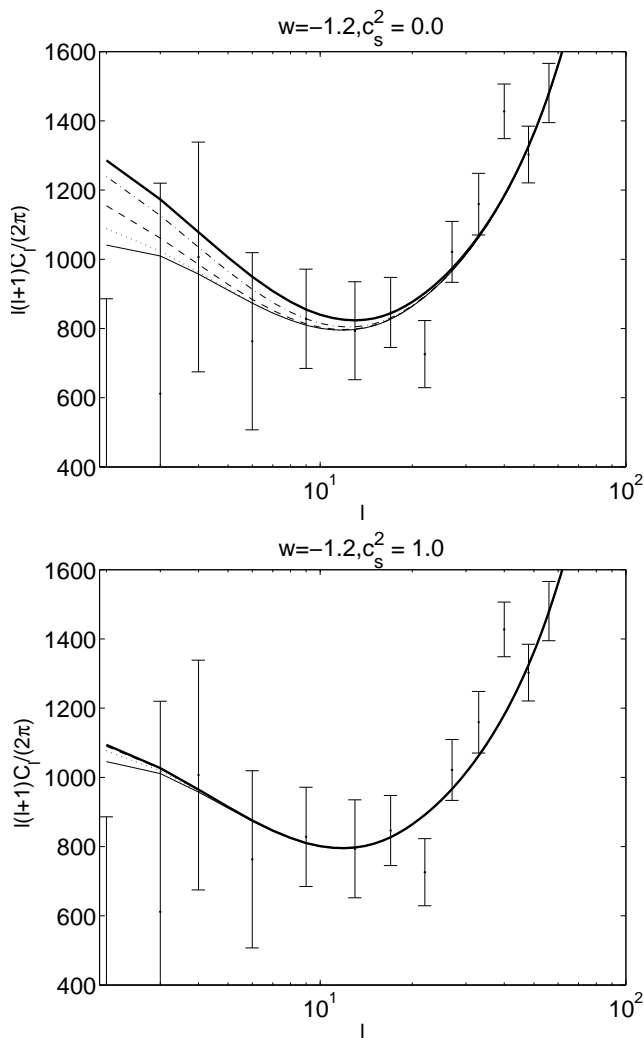


FIG. 6: The CMBR anisotropies for  $w = -1.2$ . In the upper panel  $c_s^2 = 0$  and in the lower panel  $c_s^2 = 1.0$ . The ISW contribution decreases with the parameter  $c_{vis}^2$ : thick lines are for  $c_{vis}^2 = 0$ , dash-dotted lines for  $c_{vis}^2 = 0.001$ , dashed lines for  $c_{vis}^2 = 0.01$ , dotted lines for  $c_{vis}^2 = 0.1$  and the solid lines for  $c_{vis}^2 = 1.0$ .

formal definition does not describe propagation of waves in any physical matter. A priori one should not discard the possibility  $c_s^2 < 0$  without careful deliberation. In fact, given a fluid with negative equation of state, one would expect, from Eq. (3), also a negative sound speed squared. To get rid of this feature, extra degrees of freedom must be assumed to exist in such a way that the variable defined by Eq. (4) turns out positive.

When the generation of shear in the fluid is taken into account, the perturbation growth for  $c_s^2 < 0$  can be stabilized. This is because shear is sourced by the perturbations, and in turn the shear will inhibit clustering. Here it is possible to choose the parameters in such a way that the dark energy perturbation grows steadily at late times. So the ISW effect comes with the opposite sign from the

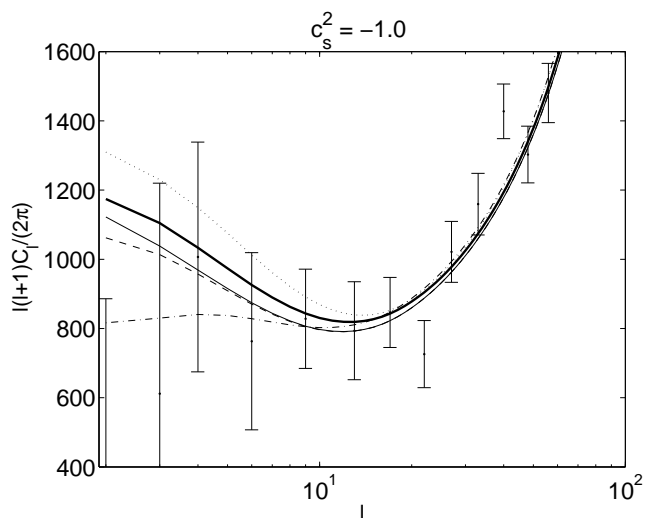


FIG. 7: The CMBR spectra for  $c_s^2 = -1.0$ . The thick line is for  $w = -1$  (unperturbed dark energy). The solid line is for  $w = -0.8$  and  $c_{vis}^2 = 0.5$  and the dash-dotted line for  $w = -0.8$  and  $c_{vis}^2 = 1.0$ . The dotted line is for  $w = -1.2$  and  $c_{vis}^2 = 0.5$  and the dashed line for  $w = -1.2$  and  $c_{vis}^2 = 1.0$ .

Sachs-Wolfe effect, which leaves its imprint in the CMBR earlier. These effects cancel each other and thus the large scale power in the CMBR spectrum is reduced, in accordance with the measured low quadrupole. We show in FIG. 7 such a case together with various other choices for the other two parameters when  $c_s^2 = -1$ .

#### D. A summary

We summarize the features of dark energy perturbations in different parameter regions in Table I. A half of the parameter space is excluded because divergent behaviour occurs, and much of the remaining parameter space is degenerated. Even when restricting to simplest case where the parameters are kept constant, it seems clear that present observational data allows large variety of interesting models with non-vanishing shear,  $c_{vis}^2 \neq 0$ . In some parameter regions of Table I new features appear at observable scales.

In FIG. 8 we plot the matter power spectra including cold dark matter and baryons for various parameter choices. When  $c_{vis}^2$  is varied, the effect occurs only at scales much larger than what current observations are able to probe. In the spectrum of the total density perturbation one would see more pronounced features at scales more tantalizingly near the current limits of observations. However, there is no way to directly measure the dark energy density perturbation, and therefore we have plotted only the power spectrum of non-relativistic matter.

In FIG. 2 and FIG. 5 it was seen that the shear changes the Newtonian gravitational potentials signifi-

$w$	$c_s^2$	$c_{vis}^2 < 0$	$c_{vis}^2 = 0$	$c_{vis}^2 > 0$
$> -1$	$> 0$	diverges	canonic scalar field	$\searrow$ (FIG. 3)
	$< 0$	diverges	diverges	$\nearrow$ † (FIG. 7)
$< -1$	$> 0$	$\nearrow$ (FIG. 6)	phantom scalar field	diverges
	$< 0$	$\searrow$ † (FIG. 7)	diverges	diverges

TABLE I: Summary of different parameter regions for dark energy fluids. We have indicated with  $\nearrow$  the cases where superhorizon perturbations are increased as  $|c_{vis}^2|$  is increased, and with  $\searrow$  the cases where superhorizon perturbations in dark energy are smoothed as  $c_{vis}^2$  is increased. We indicate by † that the shear perturbation influences significantly also the small scale perturbations.

cantly. Thus one might hope to find a way to study whether effects from an anisotropic stress could be measured by using for example the cross correlation of the ISW signal and the large scale structure observations or gravitational lensing experiments. However, one should keep in mind that we have considered perturbations at vast scales. We have found that that fluctuations in an imperfect as well as in a perfect fluid with a constant equation of state  $w < -1/3$  are confined to superhorizon scales. This is except for special occasions, in particular when the parameter  $c_s^2$  is negative or when the perturbations behave pathologically due to wrong sign of the viscous parameter. For the largest scales, the viscous parameter determines the evolution of the perturbations. It is clear from FIG. (1) and FIG. (4) that the variation of the sound speed  $c_s^2$  has much less effect on the evolution of perturbations in the limit  $k \rightarrow 0$ . However, the parameter  $c_s^2$  sets the scale at which the fluctuations in dark energy become negligible. For smaller  $c_s^2$ , there are fluctuations at smaller wavelengths. Therefore the shear would be best seen when the  $c_s^2$  is nearly zero or even negative.

The main impact of dark energy anisotropic stress on observations seems to be the modification of the CMBR at very large scales, from which it would be very difficult to unambiguously detect. However, this changes when one considers the perhaps better physically motivated situation where the parameters  $w$ ,  $c_s^2$  and  $c_{vis}^2$  are allowed to evolve in time.

#### IV. IMPERFECT UNIFIED MODELS

The Chaplygin gas [66] is a prototype of a unified model of dark matter and dark energy [67]. In such models a single energy component accounts for both the dark matter and dark energy. Thus this component must resemble cold dark matter in the earlier universe, whereas it should exhibit large negative pressure nowadays. These models are, however, problematic because of the suppression of structure formation by the adiabatic pressure perturbations [39]. A solution for this problem has been based on the observation that due to entropy, the sound

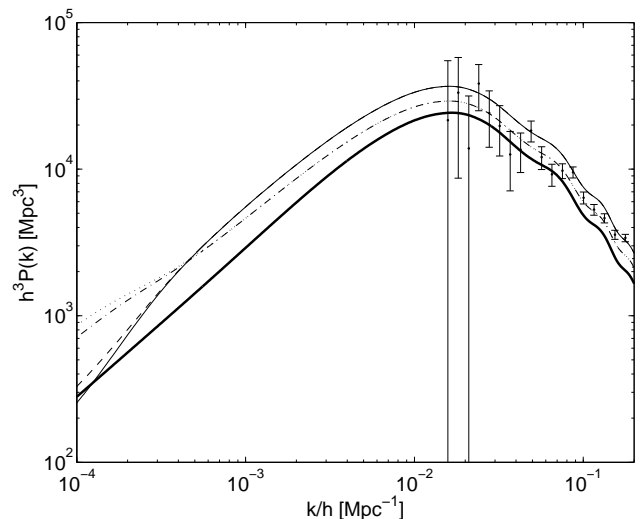


FIG. 8: The total matter power spectra when  $c_{vis}^2 = 1.0$ . The thick line is for  $w = -0.8$  and  $c_s^2 = 1.0$ . The dash-dotted line for  $w = -0.8$  and  $c_s^2 = 0$ , the dotted line for  $w = -0.8$  and  $c_s^2 = 1$ . The dashed line is for  $w = -1.2$  and  $c_s^2 = 0$ , the solid line for  $w = -1.2$  and  $c_s^2 = 1$ .

speed is not necessarily the adiabatic one [33, 68, 69]. In the so called silent quartessence model entropy perturbations cancel the effect of the adiabatic sound speed [70].

The modified polytropic Cardassian expansion [71] (MPC) in the fluid interpretation [72] provides a general parameterization which encompasses a wide variety of unified models. For the MPC case, one can write the energy density as a function of the scale factor as

$$\rho = [Aa^{3q(\nu-1)} + Ba^{-3q}]^{\frac{1}{q}}. \quad (16)$$

The exponents  $q$ ,  $\nu$  are given as parameters, and the constants  $A$ ,  $B$  have the appropriate mass dimension. This parameterization is equivalent to the New Generalized Chaplygin gas [73]. When  $\nu = 2$ , one gets the Generalized Chaplygin gas [74] where  $q$  can vary, and setting further  $q = 1$ , one is left with the original Chaplygin gas [66]. On the other hand, when the parameter  $\nu$  can get any values and  $q$  is set to  $q = 2$ , the Variable Chaplygin gas [75] is recovered. Finally, when  $q = 1$  and  $\nu$  is arbitrary, one has the simplest version of the Cardassian expansion which reproduces the background expansion of a universe with standard CDM and dark energy with  $w = \nu - 2$  [76].

We will consider here effects of shear in models where the unified dark density is defined by Eq. (16). In the above references, various theoretical origins for such density ansatzes have been proposed, but we will not consider here whether these necessitate incorporation of shear in the linear order in cosmology. Previously Cardassian expansion has been studied in the modified gravity context [33], and there it was shown that an effective anisotropic stress can appear in the late universe.



With certain assumptions for the modified gravity, the cold dark matter density perturbation generates a shear perturbation algebraically determined from the density and velocity fields of the matter interestingly similarly to the case motivated by the covariant generalization of the Navier-Stokes equation (7). Then the resulting matter power spectrum is in better accordance with observations than in the standard adiabatic case, but as the anisotropic stress affects the gravitational potentials and thus enhances the ISW effect, the CMBR spectrum will then restrict the allowed parameter space stringently. However, we will here consider the anisotropically stressed fluid as parameterized by Eq.(9). As expected, our results will be different from the modified gravity approach of Ref. [33].

The equation of state for the unified fluid described by Eq.(16) is

$$w = \frac{\nu A a^{3q(\nu-1)}}{A a^{3q(\nu-1)} + B a^{-3q}}, \quad (17)$$

and it follows that

$$c_a^2 = \frac{w [1 - \nu q + w(1 - q)]}{1 + w}. \quad (18)$$

When both  $q$  and  $\nu$  are equal to one, the model is equivalent to cold dark matter and a cosmological constant. When either  $q$  or  $\nu$  is smaller than one,  $c_a^2$  will be negative in the late universe, and when either  $q$  or  $\nu$  is greater than one, the  $c_s^2$  will stay positive and grow in the late universe. For instance, if  $\nu = 1$ , the asymptotic value is  $c_s^2 = 1 - q$ .

In the adiabatic case then  $c_s = c_a$ , but for the silent quartessence one imposes a special condition on  $c_s^2$ , namely that the pressure perturbation vanishes in the synchronous gauge [68, 70]. Here we consider the case that all the three sound speeds are equal in magnitude, including the viscosity parameter as it appears in Eq. (9). Thus  $c_{vis}^2 = |c_a^2|$  and  $c_s^2 = c_a^2$ . This seems a natural generalization of the characteristics of better known cosmic fluids, i.e. neutrinos. Then, in the terminology employed here, the fluid is adiabatic but imperfect<sup>2</sup>. For comparison, we include also results for the silent quartessence, as an example of an entropic but perfect fluid. In addition, results for the adiabatic and perfect model are shown.

We plot the results for the CMBR spectrum in FIG. 9, and for the matter power spectra in FIG. 10 and FIG. 11. Here the matter power spectra include all the components in the energy budget, since one cannot distinguish dark matter from the unified model. In all the figures, the adiabatic case is shown with dash-dotted lines, the entropic case with dashed lines and the imperfect case with solid lines.

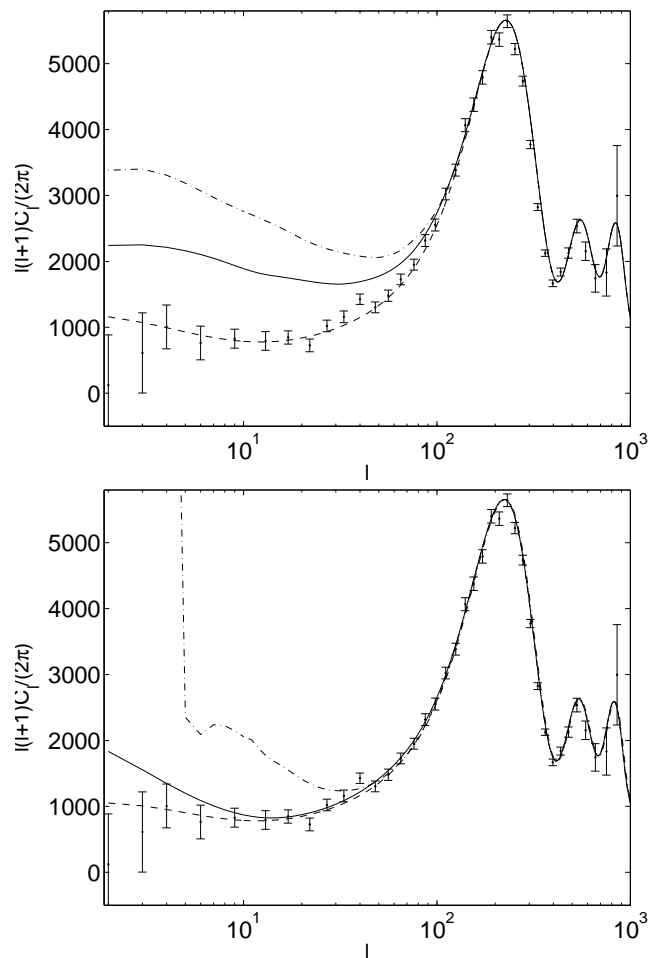


FIG. 9: The CMBR anisotropies for the MPC model with  $q = 1.0$ . The dash-dotted lines are for the adiabatic case, the solid lines for the same model with the shear included, and the dashed lines correspond to the silent case. In the upper panel  $\nu = 1.1$ . In the lower panel  $\nu = 0.9$  for the silent and the imperfect case. The adiabatic model has  $\nu = 0.994$ , which already gives disproportionately large ISW effect.

The effect of shear is to stabilize the perturbations. When  $q$  or  $\nu$  is greater than one, the adiabatic pressure tends to drive the density perturbation to oscillate. However, including the anisotropic stress will remove the oscillations, since the damping effect of shear compensates steep gradients. The overall suppression of growth is alleviated, but not as much as in the silent model. When either  $q$  or  $\nu$  is smaller than one, the adiabatic pressure would drive the density perturbation to a very fast growth. However, as discussed in the previous section, the shear viscosity eliminates this driving force.

## V. CONCLUSIONS

In this article we have investigated the effects of an anisotropic stress in the dark energy component on large

<sup>2</sup> The presence of anisotropic stress does not lead to generation of entropy at the linear order [77].

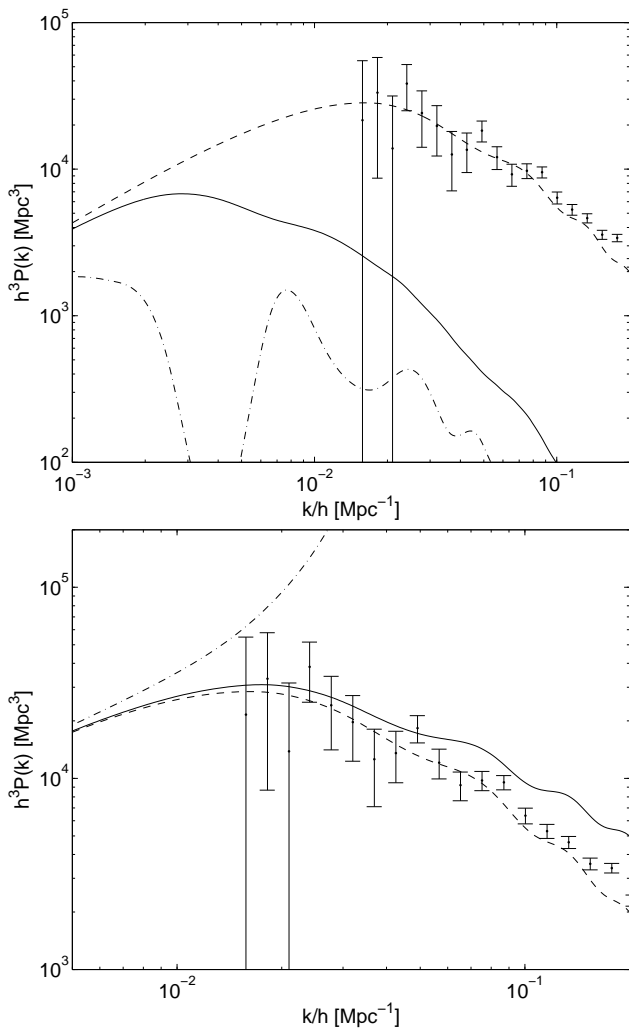


FIG. 10: The total matter power spectra for MPC model when  $\nu = 1.0$ . In the upper panel  $\nu = 1.01$ , and in the lower panel  $\nu = 0.999$ .

scale structures.

We have parameterized the dark energy component with three variables. The equation of state determines the decay rate of dark energy, and the sound speed characterizes the evolution of its fluctuations. These two were treated as independent parameters, thus accounting for possible entropy in the fluid. In addition we allowed for shear viscosity in the linear order. We discussed the possibility to apply a Navier-Stokes type viscosity to determine the additional degree of freedom for dark energy fluctuations, the amount of shear viscosity, but we adopted the parameterization utilizing a viscosity parameter  $c_{vis}^2$ , motivated by the fact that it seems to generalize the familiar and well understood cosmological fluids in a natural way [62].

Using this phenomenological three parameter fluid description we investigated the effect of an imperfect dark energy fluid and of unified dark matter and dark energy

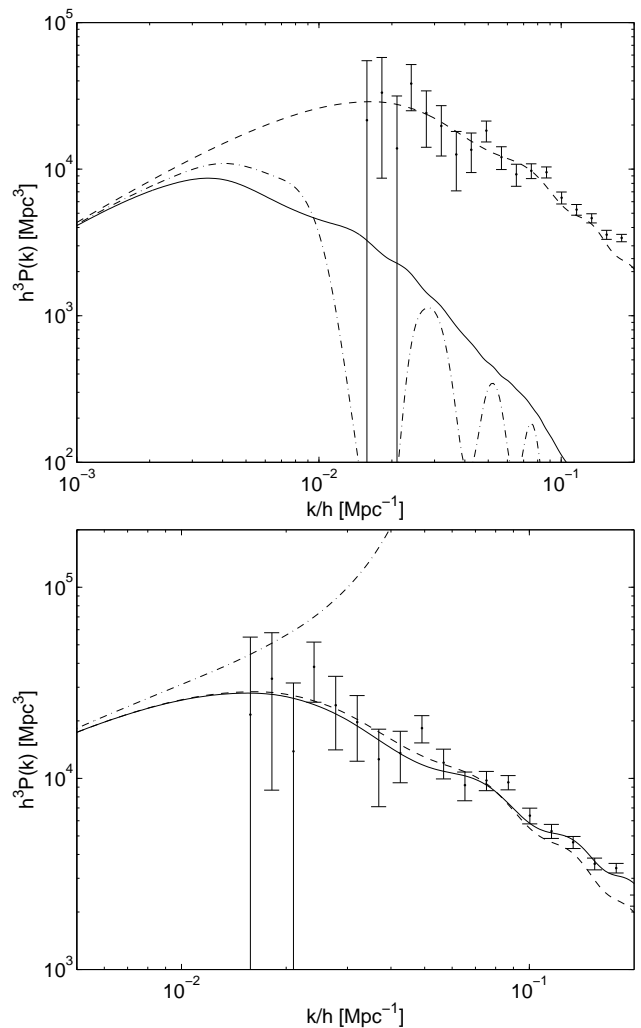


FIG. 11: The total matter power spectra for MPC model when  $\nu = 1.0$ . In the upper panel  $q = 1.01$ , and in the lower panel  $q = 0.999$ .

models on the matter power spectrum and on the CMBR temperature anisotropies. For most models we find that free streaming effects tend to smooth density fluctuations. However, there are some exceptions, described below.

In dark energy models where  $-1 \leq w < 0$ , we found that increasing the anisotropic stress results in a swifter decay of dark energy overdensities, which is seen in the CMBR spectrum as an amplification of the ISW effect. The opposite occurs in the case of phantom dark energy ( $w < -1$ ), for which the anisotropic stress supports the growth of overdensities and thus reduces the ISW effect. However, the impact of anisotropic stress on the CMBR spectrum can be closely mimicked by varying the sound speed of dark energy. This makes it difficult to distinguish between these two fluid properties.

In addition, we found that negative sound speeds are also consistent with observations, if shear viscosity is in-

cluded. The situation that the pressure perturbation (evaluated in the comoving frame) is of the opposite sign than the density perturbation, is formally unproblematical to define, but when  $c_{vis}^2 = 0$  it will exhibit unlimited growth of density fluctuations. However, when  $c_{vis}^2 > 0$  this does not occur. For a suitable choice of parameters a low amplitude for the CMBR quadrupole is produced, in accordance with observations.

In models unifying dark matter and dark energy extended with shear, it is found that the anisotropic stress can stabilize the effect of the adiabatic pressure perturbation, thus slightly improving the compatibility of these models with large scale structure observations. It remains to be seen how one can loosen the constraints by allowing for an anisotropic stress. Our main objective here was to use these models as examples of dark energy with evolving  $w$ ,  $c_s$  and  $c_{vis}$ . The conclusion taken is that, in contrast to the simplest fluid models with constant  $w$ ,  $c_s$  and  $c_{vis}$ , in specific scenarios the shear stress can have consequences distinguishable with present ob-

servational data.

In general, we found that anisotropic perturbations in dark energy is an interesting possibility which is not excluded by the present day observational data. Furthermore, we found that the CMBR large scale temperature fluctuations, due to the the ISW effect, are a promising tool to constrain the possible imperfectness of the dark energy component. Even when the anisotropic stress cannot be directly measured, it can still bias measurements of other parameters, for instance the dark energy speed of sound or its equation of state.

### Acknowledgments

We thank H. Kurki-Suonio for useful discussions. TK is supported by Magnus Ehrnrooth Foundation. DFM acknowledge support from the Research Council of Norway through project number 159637/V30.

- 
- [1] A. G. Riess et al. (Supernova Search Team), *Astron. J.* **116**, 1009 (1998), astro-ph/9805201.
  - [2] S. Perlmutter et al. (Supernova Cosmology Project), *Astrophys. J.* **517**, 565 (1999), astro-ph/9812133.
  - [3] A. G. Riess et al. (Supernova Search Team), *Astrophys. J.* **607**, 665 (2004), astro-ph/0402512.
  - [4] M. Tegmark et al. (SDSS), *Phys. Rev.* **D69**, 103501 (2004), astro-ph/0310723.
  - [5] M. Colless (1998), astro-ph/9804079.
  - [6] D. N. Spergel et al. (WMAP), *Astrophys. J. Suppl.* **148**, 175 (2003), astro-ph/0302209.
  - [7] S. M. Carroll, *Living Rev. Rel.* **4**, 1 (2001), astro-ph/0004075.
  - [8] C. Wetterich, *Astron. Astrophys.* **301**, 321 (1995), hep-th/9408025.
  - [9] B. Ratra and P. J. E. Peebles, *Phys. Rev.* **D37**, 3406 (1988).
  - [10] R. R. Caldwell, R. Dave, and P. J. Steinhardt, *Phys. Rev. Lett.* **80**, 1582 (1998), astro-ph/9708069.
  - [11] I. Zlatev, L.-M. Wang, and P. J. Steinhardt, *Phys. Rev. Lett.* **82**, 896 (1999), astro-ph/9807002.
  - [12] L. Amendola, *Phys. Rev.* **D62**, 043511 (2000), astro-ph/9908023.
  - [13] G. R. Farrar and P. J. E. Peebles, *Astrophys. J.* **604**, 1 (2004), astro-ph/0307316.
  - [14] A. W. Brookfield, C. van de Bruck, D. F. Mota, and D. Tocchini-Valentini (2005), astro-ph/0503349.
  - [15] J. S. Bagla, H. K. Jassal, and T. Padmanabhan, *Phys. Rev.* **D67**, 063504 (2003), astro-ph/0212198.
  - [16] T. Padmanabhan, *Phys. Rev.* **D66**, 021301 (2002), hep-th/0204150.
  - [17] C. Armendariz-Picon, V. Mukhanov, and P. J. Steinhardt, *Phys. Rev.* **D63**, 103510 (2001), astro-ph/0006373.
  - [18] O. Bertolami and D. F. Mota, *Phys. Lett.* **B455**, 96 (1999), gr-qc/9811087.
  - [19] B. Boisseau, G. Esposito-Farese, D. Polarski, and A. A. Starobinsky, *Phys. Rev. Lett.* **85**, 2236 (2000), gr-qc/0001066.
  - [20] R. R. Caldwell, *Phys. Lett.* **B545**, 23 (2002), astro-ph/9908168.
  - [21] G. W. Gibbons, *Class. Quant. Grav.* **20**, S321 (2003), hep-th/0301117.
  - [22] T. Chiba, T. Okabe, and M. Yamaguchi, *Phys. Rev.* **D62**, 023511 (2000), astro-ph/9912463.
  - [23] U. Seljak et al., *Phys. Rev.* **D71**, 103515 (2005), astro-ph/0407372.
  - [24] D. F. Mota and J. D. Barrow, *Phys. Lett.* **B581**, 141 (2004), astro-ph/0306047.
  - [25] A. K. D. Evans, I. K. Wehus, O. Gron, and O. Elgaroy, *Astron. Astrophys.* **430**, 399 (2005), astro-ph/0406407.
  - [26] M. Manera and D. F. Mota (2005), astro-ph/0504519.
  - [27] M. Amarguioui, O. Elgaroy, and T. Multamaki, *JCAP* **0501**, 008 (2005), astro-ph/0410408.
  - [28] U. Alam, V. Sahni, T. D. Saini, and A. A. Starobinsky, *Mon. Not. Roy. Astron. Soc.* **354**, 275 (2004), astro-ph/0311364.
  - [29] D. F. Mota and J. D. Barrow, *Mon. Not. Roy. Astron. Soc.* **349**, 281 (2004), astro-ph/0309273.
  - [30] A. Melchiorri, L. Mersini-Houghton, C. J. Odman, and M. Trodden, *Phys. Rev.* **D68**, 043509 (2003), astro-ph/0211522.
  - [31] D. F. Mota and C. van de Bruck, *Astron. Astrophys.* **421**, 71 (2004), astro-ph/0401504.
  - [32] S. Hannestad and E. Mortsell, *Phys. Rev.* **D66**, 063508 (2002), astro-ph/0205096.
  - [33] T. Koivisto, H. Kurki-Suonio, and F. Ravndal, *Phys. Rev.* **D71**, 064027 (2005), astro-ph/0409163.
  - [34] N. J. Nunes and D. F. Mota (2004), astro-ph/0409481.
  - [35] T. Koivisto, *Phys. Rev.* **D72**, 043516 (2005), astro-ph/0504571.
  - [36] W. Hu and D. J. Eisenstein, *Phys. Rev.* **D59**, 083509 (1999), astro-ph/9809368.
  - [37] P. J. E. Peebles and B. Ratra, *Rev. Mod. Phys.* **75**, 559 (2003), astro-ph/0207347.
  - [38] R. Bean and O. Dore, *Phys. Rev.* **D69**, 083503 (2004),

- astro-ph/0307100.
- [39] H. Sandvik, M. Tegmark, M. Zaldarriaga, and I. Waga, *Phys. Rev.* **D69**, 123524 (2004), astro-ph/0212114.
- [40] P. P. Avelino, L. M. G. Beca, J. P. M. de Carvalho, C. J. A. P. Martins, and P. Pinto, *Phys. Rev.* **D67**, 023511 (2003), astro-ph/0208528.
- [41] A. B. Balakin, D. Pavon, D. J. Schwarz, and W. Zimdahl, *New. J. Phys.* **5**, 085 (2003), astro-ph/0302150.
- [42] C. Armendariz-Picon, *JCAP* **0407**, 007 (2004), astro-ph/0405267.
- [43] V. V. Kiselev, *Class. Quant. Grav.* **21**, 3323 (2004), gr-qc/0402095.
- [44] W. Zimdahl, D. J. Schwarz, A. B. Balakin, and D. Pavon, *Phys. Rev.* **D64**, 063501 (2001), astro-ph/0009353.
- [45] M. Novello, S. E. Perez Bergliaffa, and J. Salim (2003), astro-ph/0312093.
- [46] H. Wei and R.-G. Cai (2006), astro-ph/0603052.
- [47] J. D. Barrow (1997), gr-qc/9712020.
- [48] E. F. Bunn, P. Ferreira, and J. Silk, *Phys. Rev. Lett.* **77**, 2883 (1996), astro-ph/9605123.
- [49] T. R. Jaffe, A. J. Banday, H. K. Eriksen, K. M. Gorski, and F. K. Hansen, *Astrophys. J.* **629**, L1 (2005), astro-ph/0503213.
- [50] P. Bielewicz, K. M. Gorski, and A. J. Banday, *Mon. Not. Roy. Astron. Soc.* **355**, 1283 (2004), astro-ph/0405007.
- [51] D. L. Larson and B. D. Wandelt, *Astrophys. J.* **613**, L85 (2004), astro-ph/0404037.
- [52] D. J. Schwarz, G. D. Starkman, D. Huterer, and C. J. Copi, *Phys. Rev. Lett.* **93**, 221301 (2004), astro-ph/0403353.
- [53] C. J. Copi, D. Huterer, and G. D. Starkman, *Phys. Rev.* **D70**, 043515 (2004), astro-ph/0310511.
- [54] A. de Oliveira-Costa, M. Tegmark, M. Zaldarriaga, and A. Hamilton, *Phys. Rev.* **D69**, 063516 (2004), astro-ph/0307282.
- [55] I. Brevik, S. Nojiri, S. D. Odintsov, and L. Vanzo, *Phys. Rev.* **D70**, 043520 (2004), hep-th/0401073.
- [56] I. Brevik, O. Gorbunova, and Y. A. Shaido (2005), gr-qc/0508038.
- [57] S. Nojiri and S. D. Odintsov, *Phys. Rev.* **D72**, 023003 (2005), hep-th/0505215.
- [58] I. Brevik and O. Gorbunova (2005), gr-qc/0504001.
- [59] C.-P. Ma and E. Bertschinger, *Astrophys. J.* **455**, 7 (1995), astro-ph/9506072.
- [60] S. Hannestad, *Phys. Rev.* **D71**, 103519 (2005), astro-ph/0504017.
- [61] C. Misner, Thorne, K. S., and J. Wheeler, *GRAVITATION* (W.H. Freeman and Company, 1970).
- [62] W. Hu, *Astrophys. J.* **506**, 485 (1998), astro-ph/9801234.
- [63] G. Huey (2004), astro-ph/0411102.
- [64] A. Lewis, A. Challinor, and A. Lasenby, *Astrophys. J.* **538**, 473 (2000), astro-ph/9911177.
- [65] J. Weller and A. M. Lewis, *Mon. Not. Roy. Astron. Soc.* **346**, 987 (2003), astro-ph/0307104.
- [66] A. Y. Kamenshchik, U. Moschella, and V. Pasquier, *Phys. Lett.* **B511**, 265 (2001), gr-qc/0103004.
- [67] N. Bilic, G. B. Tupper, and R. D. Viollier, *Phys. Lett.* **B535**, 17 (2002), astro-ph/0111325.
- [68] R. R. R. Reis, I. Waga, M. O. Calvao, and S. E. Joras, *Phys. Rev.* **D68**, 061302 (2003), astro-ph/0306004.
- [69] W. Zimdahl and J. C. Fabris, *Class. Quant. Grav.* **22**, 4311 (2005), gr-qc/0504088.
- [70] L. Amendola, I. Waga, and F. Finelli (2005), astro-ph/0509099.
- [71] K. Freese, *Nucl. Phys. Proc. Suppl.* **124**, 50 (2003), hep-ph/0208264.
- [72] P. Gondolo and K. Freese, *Phys. Rev.* **D68**, 063509 (2003), hep-ph/0209322.
- [73] X. Zhang (2004), astro-ph/0411221.
- [74] M. C. Bento, O. Bertolami, and A. A. Sen, *Phys. Rev.* **D66**, 043507 (2002), gr-qc/0202064.
- [75] Z.-K. Guo and Y.-Z. Zhang (2005), astro-ph/0506091.
- [76] K. Freese and M. Lewis, *Phys. Lett.* **B540**, 1 (2002), astro-ph/0201229.
- [77] R. Maartens and J. Triginer, *Phys. Rev.* **D56**, 4640 (1997), gr-qc/9707018.